JOURNAL OF COMPUTATIONAL PHYSICS 6, 288–313 (1970)

Numerical Evaluation of the Slab Albedo Problem Solution in One-Speed Anisotropic Transport Theory*

HANS G. KAPER,† J. KENNETH SHULTIS,‡ AND JAAP G. VENINGA§

Department of Mathematics, University of Groningen, Groningen, the Netherlands

Received January 7, 1970; revised April 13, 1970

In this paper the normal mode expansion technique is employed to obtain numerical results for the solution of the slab albedo problem in one-speed transport theory with anisotropic scattering. Methods are presented by which one may compute the angular distribution of particles anywhere in a slab of finite thickness for any degree of anisotropy of the scattering function. Many numerical examples are given and, from these examples, it is demonstrated how the slab albedo problem solution varies with the problem parameters, viz., the degree of anisotropy of the scattering function, the angle of incidence of the source beam, the slab thickness and the multiplication factor.

I. INTRODUCTION

In the last ten years the singular eigenfunction or normal mode expansion technique, as developed by Lafore and Millot [1] and Case [2, 3], has been widely applied to one-speed transport problems in systems with plane symmetry. While most of the investigations have been limited to problems in infinite or semiinfinite media, some authors have applied this technique successfully to problems in slabs of finite thickness, assuming that the phase function for single scattering is isotropic [4–7]. Recently, Kaper has extended these results to anisotropically scattering media in a study of the slab albedo problem [8].

The applicability of these results to practical problems of particle transport has been hampered by the extreme difficulties that are encountered in reducing the analytical expressions to numerics. A fundamental difficulty inherent in all slab problems is that the coefficients in the eigenfunction expansion do not follow from the theory in a closed form but, rather, they are defined by the solution of a set of coupled Fredholm integral equations. When the phase function for single scattering

* This work was partially supported by the Netherlands Organization for the Advancement of Pure Research (Z.W.O.).

† Present address: Applied Mathematics Division, Argonne National Laboratory, Argonne, Illinois.

‡ Present address: Nuclear Engineering Dept., Kansas State University, Manhattan, Kansas.

§ Present address: Computing Center, University of Groningen, Groningen, the Netherlands.

is highly anisotropic—a situation often encountered in physical problems—many additional computational problems arise. Several of the special functions which are well defined by the theory, become exceedingly difficult to evaluate numerically. Often, the computer is unable to perform computations with sufficient accuracy to give meaningful results from straightforward evaluations of some of these special functions from their definitions and a very careful numerical analysis must be performed. The fact that the normal mode expansion technique gives rise to expressions involving singular integrals, many of which have rapidly varying integrands, further complicates its application in practical situations.

The primary purpose of the present paper, therefore, is to investigate the various numerical problems inherent in the singular eigenfunction expansion technique as applied to anisotropic transport problems in a slab. Such an investigation is a prerequisite if this method is ever to be useful as a practical computational method of solving transport problems. In particular, we consider the slab albedo problem, which is the fundamental slab problem since the solution to any transport problem in a slab may be expressed as a linear combination of various slab albedo problem solutions and the simpler infinite medium problem solutions—see, e.g. [9].

The present computational study of the slab albedo problem does have an immediate practical aspect. Generally, it is impossible to see from the theoretical results, even qualitatively, how the solution varies with the problem parameters (e.g., the degree of anisotropy of the scattering function, the slab thickness, the angle of incidence of the source beam, the multiplication factor). The dependence of the solution upon the problem parameters can be found only by a numerical evaluation. Finally, the numerical results presented in this paper provide a means of checking the validity of certain approximation schemes used in practical problems of particle transport in matter, e.g., in neutron transport theory and in radiative transfer.

The general plan of the paper is as follows. After a formulation of the slab albedo problem in Section II, we briefly review in Section III the singular eigenfunction technique and the exact analytical solution to the slab albedo problem as given by Kaper [8]. Then, in Section IV, we discuss some of the numerical difficulties in the evaluation of this solution and present methods whereby these difficulties may be overcome. Finally, in Section V, we give several numerical examples and show how the albedo problem solution varies with the problem parameters.

II. Formulation of the Problem

Consider a homogeneous, isotropic, source-free medium which is infinite in the y and z directions and occupies the region $0 \leqslant x \leqslant d$ in space. The medium is surrounded by vacuum on both sides. An azimuthally symmetric beam of particles

is incident upon the free surface $x = 0$. Inside the medium, all particles are assumed to travel with the same speed and to be scattered anisotropically. The mean number of secondaries per collision is denoted by c. Further, since the medium has been assumed isotropic, the angular density of the particles inside the medium is azimuthally symmetric. Thus, if we measure distance, x, in units of the mean free path and measure direction by the cosine, μ, of the angle between the velocity vector and the positive x axis, the angular distribution, ψ, of particles inside the medium obeys the equation [3]

$$\mu \frac{\partial \psi}{\partial x} + \psi(x, \mu) = \frac{c}{2} \int_{-1}^{1} d\mu' f(\mu', \mu) \psi(x, \mu') \tag{2-1}$$

for $0 \leqslant x \leqslant d$, $-1 \leqslant \mu \leqslant 1$, together with the boundary conditions

$$\psi(0, \mu) = \Psi(\mu), \qquad 0 < \mu \leqslant 1 \tag{2-2}$$

and

$$\psi(d, \mu) = 0, \qquad -1 \leqslant \mu < 0, \tag{2-3}$$

where Ψ represents the angular distribution of the incident source beam. In Eq. (2-1), f is the phase function for single scattering averaged over the azimuthal angle, i.e.,

$$f(\mu', \mu) = \frac{1}{2\pi} \int_{0}^{2\pi} d\varphi' f(\boldsymbol{\Omega}' \cdot \boldsymbol{\Omega}), \tag{2-4}$$

where $\boldsymbol{\Omega}'$ and $\boldsymbol{\Omega}$ are, respectively, the unit vectors in the direction of the velocity of a particle before and after a collision, $\boldsymbol{\Omega} \equiv (\cos^{-1}\mu, \varphi)$, $\boldsymbol{\Omega}' \equiv (\cos^{-1}\mu', \varphi')$. Normalization is such that

$$\frac{1}{4\pi} \int_{-1}^{1} d\mu' \int_{0}^{2\pi} d\varphi' f(\boldsymbol{\Omega}' \cdot \boldsymbol{\Omega}) = 1. \tag{2-5}$$

It will be assumed that f can be expanded in a finite sum of Legendre polynomials,

$$f(\boldsymbol{\Omega}' \cdot \boldsymbol{\Omega}) = \sum_{n=0}^{N} b_n P_n(\boldsymbol{\Omega}' \cdot \boldsymbol{\Omega}), \tag{2-6}$$

where the b_n's are given constants, and $b_0 = 1$. Then, using the addition theorem for Legendre polynomials, one verifies that

$$f(\mu', \mu) = \sum_{n=0}^{N} b_n P_n(\mu') P_n(\mu). \tag{2-7}$$

It is asked to find the angular density, ψ, and the first two moments of ψ, i.e., the scalar density, ρ,

$$\rho(x) = \int_{-1}^{1} \psi(x, \mu)\, d\mu, \tag{2-8}$$

and the net current, j,

$$j(x) = \int_{-1}^{1} \mu\psi(x, \mu)\, d\mu, \tag{2-9}$$

anywhere inside the slab and at the free surfaces.

III. The Slab Albedo Problem Solution

In this section we briefly outline the method by which the exact solution to the slab albedo problem may be derived and summarize the results obtained by Kaper [8].

If the homogeneous transport equation (2-1) is formally written as $(\partial\psi/\partial x) = A\psi$, the transport operator A is defined by

$$(A\varphi)(\mu) = -\mu^{-1}\left\{\varphi(\mu) - \frac{c}{2}\int_{-1}^{1} d\mu'\, f(\mu', \mu)\, \varphi(\mu')\right\} \tag{3-1}$$

for all φ belonging to the domain of A. In the normal mode expansion technique one seeks a set of solutions, $\{\varphi_\nu\}$, to the eigenvalue problem $A\varphi_\nu = \nu^{-1}\varphi_\nu$. From Eqs. (2-1), (2-7) and (3-1) it is found that the eigenvalue equation is

$$(\nu - \mu)\, \varphi(\nu, \mu) = \tfrac{1}{2}c\nu\, D(\nu, \mu), \tag{3-2}$$

where

$$D(\nu, \mu) = \sum_{n=0}^{N} b_n h_n(\nu)\, P_n(\mu) \tag{3-3}$$

and

$$h_n(\nu) = \int_{-1}^{1} d\mu'\, P_n(\mu')\, \varphi(\nu, \mu'). \tag{3-4}$$

In these equations we have written $\varphi(\nu, \mu)$, instead of $\varphi_\nu(\mu)$.

With the aid of the recurrence relation for the Legendre polynomials it is easily

verified that all h_n contain h_0 as a multiplicative factor. Since the eigenvalue problem (3-2) is homogeneous, we may normalize the functions φ by choosing

$$\int_{-1}^{1} d\mu\, \varphi(\nu, \mu) = 1. \tag{3-5}$$

With this normalization, the functions h_n can be defined alternatively by the recurrence relation

$$(n+1)\, h_{n+1}(\nu) - \nu(2n + 1 - b_n c)\, h_n(\nu) + n h_{n-1}(\nu) = 0, \qquad n = 0, 1, \ldots, N, \tag{3-6}$$

and $h_0 = 1$. For each n, h_n is polynomial of degree n, with

$$h_n(-\nu) = (-1)^n\, h_n(\nu). \tag{3-7}$$

We now specify the domain of definition of the transport operator A as the space of distributions (generalized functions) with support $[-1, 1]$ on the real axis [10]. We distinguish two cases.

(i) For $\nu \in (-1, 1)$, the eigenvalue problem (3-2) admits the solution

$$\varphi(\nu, \mu) = \frac{c\nu}{2} \frac{D(\nu, \mu)}{\nu - \mu} + \lambda(\nu)\, \delta(\nu - \mu), \tag{3-8}$$

where the generalized functions $(\nu - \mu)^{-1}$ and $\delta(\nu - \mu)$ are defined by the functionals

$$\langle (\nu - \mu)^{-1}, \Phi(\mu) \rangle = \oint_{-1}^{1} d\mu \frac{\Phi(\mu)}{\nu - \mu} \tag{3-9}$$

and

$$\langle \delta(\nu - \mu), \Phi(\mu) \rangle = \begin{cases} \Phi(\nu) & \text{if } \nu \in [-1, 1] \\ 0 & \text{if } \nu \notin [-1, 1], \end{cases} \tag{3-10}$$

respectively, for all test functions Φ. The symbol $\oint$ refers to integration in the Cauchy principal value sense. Substitution of Eq. (3-8) into the normalization condition (3-5) gives the λ function as

$$\lambda(\nu) = \tfrac{1}{2}\{\Lambda^+(\nu) + \Lambda^-(\nu)\}, \tag{3-11}$$

where Λ^+ and Λ^- are the boundary values of a function Λ which is analytic in the complex plane cut along the real axis between -1 and $+1$,

$$\Lambda(z) = 1 - \frac{cz}{2} \int_{-1}^{1} d\mu \frac{D(z, \mu)}{z - \mu} \qquad z \notin [-1, 1], \tag{3-12}$$

given by the expressions

$$\Lambda^{\pm}(\nu) \equiv \Lambda(\nu \pm i0) = 1 - \frac{c\nu}{2} \oint_{-1}^{1} d\mu \frac{D(\nu, \mu)}{\nu - \mu} \pm \tfrac{1}{2}\pi i c\nu D(\nu, \nu), \quad -1 < \nu < 1. \tag{3-13}$$

(ii) For $\nu \notin [-1, 1]$, the normalization condition (3-5) leads to an implicit equation (the so-called *dispersion relation*) for the eigenvalue ν, viz.,

$$\Lambda(\nu) = 0. \tag{3-14}$$

Since Λ is an even function, Eq. (3-14) generally has $2M$ roots, $\pm\nu_j$, $j = 1,..., M$, and for the case of $c < 1$, all of these discrete eigenvalues are real [11, 12]. Corresponding to these discrete eigenvalues Eq. (3-2) yields the following eigensolutions which are of the regular type,

$$\varphi(\pm\nu_j, \mu) = \frac{c\nu_j}{2} \frac{D(\pm\nu_j, \mu)}{\nu_j \mp \mu}, \qquad j = 1,..., M. \tag{3-15}$$

For $c > 1$, the discrete roots $\pm\nu_j$ are not necessarily real and, as a consequence, many of the functions in the ensuing analysis become complex. To avoid these difficulties, we will restrict our investigation to the case of $c < 1$.

The use of the eigensolutions of the transport operator to obtain solutions of slab transport problems arises from the following important theorem:

THEOREM. *Any function Ψ defined on the interval $0 \leqslant \mu \leqslant 1$ which is Hölder continuous* [13] *on the open interval may be expanded in terms of the eigensolutions φ_ν, $0 \leqslant \nu \leqslant 1$ and φ_{ν_j}, $j = 1,..., M$, as*

$$\Psi(\mu) = \sum_{j=1}^{M} a_{+j}\varphi(\nu_j, \mu) + \int_0^1 d\nu\, A(\nu)\, \varphi(\nu, \mu), \tag{3-16}$$

where the coefficients a_{+j} and $A(\nu)$ are uniquely determined.

The proof of this theorem (commonly called the *half-range* completeness theorem) is quite lengthy and will not be given here. We mention only that it is a *constructive* existence proof for the expansion coefficients, see Kaper [8].

We now seek the solution of the slab albedo problem in the form

$$\psi(x, \mu) = \sum_{j=1}^{M} a_{+j}\varphi(\nu_j, \mu)\, e^{-x/\nu_j} + \sum_{j=1}^{M} a_{-j}\varphi(-\nu_j, \mu)\, e^{x/\nu_j} + \int_{-1}^{1} d\nu\, A(\nu)\, \varphi(\nu, \mu)\, e^{-x/\nu}, \tag{3-17}$$

where $a_{\pm j}$ and A are coefficients to be determined. It is easily verified that each term is itself a solution of the homogeneous transport equation (2-1). It is then necessary to find coefficients $a_{\pm j}$ and A such that the above expansion satisfies the boundary conditions (2-2) and (2-3). If such coefficients can be found, then by the existence and uniqueness theorems [14] for the one-speed transport equation, the expansion (3-17) gives the complete solution to the slab problem.

Kaper [8] has shown how the half-range completeness theorem and the boundary conditions (2-2) and (2-3) can be used to obtain a coupled set of Fredholm integral equations for the expansion coefficients. First, define

$$b_{\pm j} = a_{+j} \pm a_{-j} e^{d/\nu_j}, \tag{3-18}$$

$$B_{\pm}(\nu) = A(\nu) \pm A(-\nu)\, e^{d/\nu}, \qquad \nu > 0, \tag{3-19}$$

$$X(z) = (1 - z)^M \exp\left\{\frac{1}{2\pi i}\int_0^1 d\mu\, \frac{\arg \Lambda^+(\mu)}{\mu - z}\right\}, \qquad z \notin [0, 1], \tag{3-20}$$

$$\Lambda(\infty) = \prod_{l=0}^{N} \left(1 - \frac{b_l c}{2l + 1}\right), \tag{3-21}$$

$$\Pi(\mu) = \prod_{j=1}^{M} (\nu_j^2 - \mu^2), \tag{3-22}$$

$$W(\mu) = X(-\mu)\Pi(\mu)\Lambda(\infty)\{\lambda^2(\mu) + [\tfrac{1}{2}\pi c\mu D(\mu, \mu)]^2\}^{-1} \qquad 0 \leqslant \mu \leqslant 1, \tag{3-23}$$

$$\gamma(\mu) = \tfrac{1}{2}c\mu D(\mu, \mu)[X(-\mu)\Lambda(\infty)\Pi(\mu)]^{-1}, \qquad 0 \leqslant \mu \leqslant 1, \tag{3-24}$$

$$X(\mu) = \gamma(\mu)\lambda(\mu)[\tfrac{1}{2}c\mu D(\mu, \mu)]^{-1}, \qquad 0 \leqslant \mu \leqslant 1, \tag{3-25}$$

$$D^0(\nu, \mu) = [D(\nu, \nu) - D(\nu, \mu)]/(\nu - \mu), \tag{3-26}$$

$$F_z(\mu) = \left(1 - \frac{D(z, z)}{D(z, \mu)}\right) X(\mu) + \frac{D(z, z)}{D(z, \mu)}\, X(z) + \frac{z - \mu}{D(z, \mu)} \int_0^1 d\nu\, \frac{\gamma(\nu)\, D^0(\nu, \mu)}{\nu - \mu}. \tag{3-27}$$

Then the coefficients $b_{\pm j}$ and $B(\mu)$ (from which one finds the $a_{\pm j}$ and $A(\mu)$ using

Eqs. (3-18) and (3-19)) are found by solving the following set of coupled equations,

$$B_{\pm}(\mu) = W(\mu)\Big\{\oint_0^1 d\nu\, \frac{\gamma(\nu)\,\Psi(\nu)}{\mu-\nu} + \frac{\lambda(\mu)\,\gamma(\mu)\,\Psi(\mu)}{\frac{1}{2}c\mu D(\mu,\mu)}$$
$$- \sum_{j=1}^{M} b_{\pm j}[\varphi(\nu_j,\mu)\,F_{\nu_j}(\mu) \pm e^{-d/\nu_j}\varphi(-\nu_j,\mu)\,F_{-\nu_j}(\mu)]$$
$$\mp \frac{c}{2}\int_0^1 d\nu\, B_{\pm}(\nu)\, e^{-d/\nu}\,\frac{\nu D(\nu,-\mu)}{\nu+\mu}\,F_{-\nu}(\mu)$$
$$+ \int_0^1 d\nu\,\nu B_{\pm}(\nu)\Big[\frac{D^0(\nu,\mu)\,\lambda(\mu)\,\gamma(\mu)}{\mu D(\mu,\mu)}$$
$$+ \frac{c}{2}\oint_0^1 d\xi\,\frac{\gamma(\xi)\,D^0(\nu,\xi)}{\mu-\xi}\Big]\Big\}, \qquad 0 \leqslant \mu \leqslant 1 \tag{3-28}$$

and

$$\sum_{j=1}^{M} b_{\pm j}\Big\{\int_0^1 d\mu\,\mu^k\gamma(\mu)\,\varphi(\nu_j,\mu) \pm e^{-d/\nu_j}\int_0^1 d\mu\,\mu^k\gamma(\mu)\,\varphi(-\nu_j,\mu)\Big\}$$
$$= \int_0^1 d\mu\,\mu^k\gamma(\mu)\,\Psi(\mu) \mp \frac{c}{2}\int_0^1 d\nu\, B_{\pm}(\nu)\, e^{-d/\nu}\int_0^1 d\mu\,\mu^k\gamma(\mu)\,\frac{\nu D(\nu,-\mu)}{\nu+\mu}$$
$$+ \frac{c}{2}\int_0^1 d\nu\,\nu B_{\pm}(\nu)\int_0^1 d\mu\,\mu^k\gamma(\mu)\,D^0(\nu,\mu), \qquad k = 0, 1, \ldots, M-1. \tag{3-29}$$

Thus, since this set of equations admits a unique solution $b_{\pm j}$, $B_{\pm}(\mu)$, the albedo problem in slabs with anisotropic scattering is solved, at least formally.

IV. Numerical Evaluation

We now turn to a discussion of the main difficulties that are encountered in the numerical evaluation of the slab albedo problem solution as found in the previous section.

A. *Calculation of the Number of Pairs of Discrete Eigenvalues, M*

The number M is found from the relation

$$M = \frac{1}{\pi}\,[\Delta \arg \Lambda^{+}(\mu)]_{0\to 1}\,, \tag{4-1}$$

which is readily established from the argument principle [3, 8]. Here,

$[\Delta \arg \Lambda^+(\mu)]_{0\to 1}$ is the change of the argument of Λ^+ as the value of μ is increased continuously from 0 to 1. From Eq. (3-13) we see that $\operatorname{Re}\Lambda^+(0) = 1$ and $\operatorname{Im}\Lambda^+(0) = 0$; hence, $\arg\Lambda^+(0) = 0$. Furthermore,

$$(d/d\mu)\operatorname{Im}\Lambda^+(\mu)|_{\mu=0} = \tfrac{1}{2}\pi c D(0,0) = \tfrac{1}{2}\pi c f(0,0),$$

which is nonnegative. Hence, Λ^+ moves into the first quadrant of the complex plane as μ increases from 0. As $\mu \to 1$, $\operatorname{Re}\Lambda^+(\mu) \to \pm\infty$ while $\operatorname{Im}\Lambda^+(\mu)$ remains finite. Usually, $\arg\Lambda^+$ changes very rapidly near $\mu = 1$ and for this reason very small μ increments must be used to follow Λ^+ as it winds around the origin. A typical subdivision of the interval [0, 1] which we found useful, is $\mu = 0(0.1)$ 0.9(0.01) 0.99(0.001)0.999(0.0001)0.9999.

B. *Calculation of the Discrete Eigenvalues,* $\pm\nu_j$

To find the M discrete eigenvalues on the positive real axis we must solve for the zeros of the function Λ, cf. Eq. (3-14). However, for high degrees of anisotropy it is very difficult to evaluate Λ from Eq. (3-12), since $D(z,\mu)$, Eq. (3-3), varies extremely rapidly for $z > 1$. (Typically, a change of 10^{-10} in z can produce a 10% change in $D(z,\mu)$).

Fortunately, a modification of the dispersion relation (3-14) which avoids such problems is easily found. In fact, it may be shown [12] that Eq. (3-14) is equivalent with

$$1 - \frac{cz}{2}\int_{-1}^{1} d\mu \frac{D(\mu,\mu)}{z-\mu} = 0 \tag{4-2}$$

or, since $D(\mu,\mu)$ is an even function of μ, with

$$1 - c\int_{0}^{1} d\mu \frac{D(\mu,\mu)}{1-(\mu/z)^2} = 0. \tag{4-3}$$

This form of the dispersion relation is readily evaluated. The function $D(\mu,\mu)$, which is calculated from Eqs. (3-3) and (3-6), may have several extrema and characteristically it often varies rapidly and changes sign near the endpoint $\mu = 1$. To allow for such behavior we have found it convenient to subdivide the interval [0, 1] into several subintervals such that the integrand in Eq. (4-3) is monotonic in each subinterval, and then to use the Gaussian ten point quadrature rule for integration over each subinterval.

Finally, the M real positive zeros $\nu_1, \ldots, \nu_M$ can be quickly found from Eq. (4-3) using the method of regula falsi [15].

C. *Calculation of* $D(\nu,\mu)$ *for* $\nu > 1$

The function $D(\nu,\mu)$ is one of the most fundamental functions of anisotropic transport theory (it has the constant value 1 in the case of isotropic scattering).

This function is defined by Eqs. (3-3) and (3-4) for ν belonging to the spectrum of the transport operator and $-1 \leqslant \mu \leqslant 1$. The analytical continuation of $D(\nu, \mu)$ for ν belonging to the whole complex plane is obtained from Eq. (3-3) by defining h_n from Eq. (3-6).

For $\nu \in [-1, 1]$, $D(\nu, \mu)$ and $h_n(\nu)$ can be evaluated without any particular numerical difficulty from Eqs. (3-3) and (3-6). However, for ν appreciably greater than unity and for large N it was found to be exceedingly difficult to evaluate $D(\nu, \mu)$ directly in this way. That such difficulties should arise is not too surprising since the n-th term in the sum of (3-3), namely $b_n P_n(\mu)\, h_n(\nu)$, is a polynomial in ν of degree n, and for large n (and $\nu > 1$) this term will become very large and change quickly. Only for ν exceedingly close to the discrete eigenvalues, ν_j, do the large terms in the sum of Eq. (3-3) add together to produce a smooth and slowly varying function of μ. For very large $N(> 20)$ the accuracy required for ν_j and the ensuing evaluation of Eq. (3-3) is often larger than that available in a computer.

Since this problem arises as a result of the decomposition of D into a sum of terms each of which varies rapidly for large ν, it is preferable to define D without recourse to the decomposition (2-7) of the scattering function. Thus, instead of Eq. (3-2), we write

$$(\nu - \mu)\, \varphi(\nu, \mu) = \frac{c\nu}{2} \int_{-1}^{1} d\mu'\, f(\mu', \mu)\, \varphi(\nu, \mu'), \tag{4-4}$$

and the definition of D becomes

$$D(\nu, \mu) = \int_{-1}^{1} d\mu'\, f(\mu', \mu)\, \varphi(\nu, \mu'). \tag{4-5}$$

For $\nu > 1$, we obtain from Eqs. (4-4) and (4-5) the following integral equation for the function D,

$$D(\nu, \mu) = \frac{c\nu}{2} \int_{-1}^{1} d\mu'\, f(\mu', \mu)\, \frac{D(\nu, \mu')}{\nu - \mu'}. \tag{4-6}$$

This integral equation has a nontrivial solution if and only if ν is equal to one of the eigenvalues, ν_j, of the transport operator. The solution defines the desired function $D(\nu_j, \mu)$, cf. [12].

After setting ν equal to ν_j, the integral equation (4-6) may be solved most conveniently by approximating the integral by quadrature. Then, evaluating Eq. (4-6) at the coordinates $\mu_1, \ldots, \mu_S$ of the quadrature rule, one obtains a set of linear algebraic equations which may be written as

$$\mathbf{FAd} = \mathbf{d}, \tag{4-7}$$

where $\mathbf{d}$ is the vector whose components are

$$d_i = D(\nu_j, \mu_i), \qquad i = 1, \ldots, S, \tag{4-8}$$

and $\mathbf{A}$ and $\mathbf{F}$ are square matrices whose elements are

$$A_{ik} = \frac{c\nu_j}{2} \frac{w_i}{\nu_j - \mu_i} \delta_{ik}, \qquad i, k = 1, \ldots, S \tag{4-9}$$

and

$$F_{ik} = f(\mu_k, \mu_i), \qquad i, k = 1, \ldots, S, \tag{4-10}$$

respectively. Here, w_i is the weight factor associated with the i-th quadrature coordinate. $\mathbf{F}$ is a symmetric matrix, $F_{ik} = F_{ki}$, and $\mathbf{A}$ is a nonnegative matrix. Hence, instead of Eq. (4-6) we consider the equivalent eigenvector problem

$$\mathbf{G}\mathbf{d}' = \lambda \mathbf{d}', \qquad \lambda = 1, \tag{4-11}$$

where $\mathbf{G}$ is a symmetric matrix,

$$\mathbf{G} = \mathbf{A}^{1/2}\mathbf{F}\mathbf{A}^{1/2} = \mathbf{G}^T \tag{4-12}$$

and $\mathbf{d}'$ is the vector

$$\mathbf{d}' = \mathbf{A}^{1/2}\mathbf{d}. \tag{4-13}$$

Thus, the values of $D(\nu_j, \mu)$ at the points $\mu = \mu_i$, $i = 1, \ldots, S$, are found by solving the eigenvector problem (4-11) by Householder's method [16] and then using Eqs. (4-8) and (4-13).

In applying this method, one must choose a specific set of quadrature ordinates $\{\mu_i\}$. This set must be large enough so as to give $D(\nu_j, \mu)$ reasonably accurately over the entire μ-interval, and yet not too large so as to make the solution of eigenvector problem (4-11) very time consuming. The latter consideration restricted us to less than 100 coordinates in the interval $-1 \leqslant \mu \leqslant 1$. On the other hand, in the evaluation of the results of anisotropic transport theory it is found that the various special functions of μ involved in the theory are needed very accurately near the end point $\mu = 1$. For these reasons we split the interval $-1 \leqslant \mu \leqslant 1$ into eight subintervals, viz., $\pm[0, 0.5]$, $\pm[0.5, 0.9]$, $\pm[0.9, 0.99]$ and $\pm[0.99, 1]$, and for each subinterval we have chosen the coordinates of a ten point Gaussian quadrature rule. This particular choice of 80 ordinates besides generating many values of D near $\mu = 1$, also gives $D(\nu_j, \mu)$ at values of μ which are immediately useful for quadrature of integrals involving the D function.

So far we have treated only the case of ν_j sufficiently greater than unity such that evaluation of $D(\nu_j, \mu)$ from Eq. (3-3) becomes very difficult. Quite often

though, many of the smaller discrete eigenvalues are very close to unity. Eq. (3-3) then can be used to find D without any of the above problems, and at the same time a substantial saving in computer time is realized. Whether to employ Eq. (4-11) or Eq. (3-3) to obtain $D(\nu_j, \mu)$ obviously depends upon the magnitude of both N and ν_j.

D. *Calculation of $X(\mu)$ and $\gamma(\mu)$*

Several indirect schemes have been used to calculate the X function for the isotropic scattering case (e.g., the iteration of a nonlinear integral equation [3]), but we have found such schemes present difficulties when the scattering becomes very anisotropic. It appears most convenient to evaluate $X(\mu)$, $\mu \notin [0, 1]$, directly from the definition, Eq. (3-20), if special care is taken in evaluating the integral. Characteristically, $\arg \Lambda^+(\mu)$ changes rapidly near the end point $\mu = 1$, in particular for small c and large M. We have found that splitting the integral in Eq. (3-20) into a sum of four integrals over the partial intervals [0, 0.5], [0.5, 0.9], [0.9, 0.99] and [0.99, 1] and evaluating each integral using ten point Gaussian quadrature, gives $X(\mu)$, $-1 \leqslant \mu \leqslant 0$, to five or six significant figures even for highly anisotropic scattering functions ($N \leqslant 60$).

Once $X(\mu)$ is known for $-1 \leqslant \mu \leqslant 0$, $\gamma(\mu)$ for $0 \leqslant \mu \leqslant 1$ is easily calculated from Eq. (3-24). This function, unlike the X function, exhibits very rapid fluctuations, particularly near $\mu = 1$; and since this function appears in many integrands of the transport theory result it is important to choose very carefully the points at which γ is evaluated. Primarily for this reason, we have chosen the fixed intervals [0, 0.5], [0.5, 0.9], [0.9, 0.99], [0.99, 1] and used their corresponding coordinates for the ten point Gaussian quadrature rule to obtain 40 points of the interval $0 \leqslant \mu \leqslant 1$ at which we calculate $X(-\mu)$ and $\gamma(\mu)$. This particular set of ordinates is also used throughout the whole of the anisotropic transport theory computations. To check the validity of this interval division for integration of the γ function, the X function can be reevaluated by integrating the γ function according to the identity [8]

$$X(z) = \int_0^1 d\mu \, \frac{\gamma(\mu)}{\mu - z}, \qquad z \notin [0, 1]. \tag{4-14}$$

In all cases for $N < 50$, the X function obtained in this manner agreed to within six significant figures with the X function as calculated directly from Eq. (3-20).

E. *Calculation of $\varphi(z, \mu) F_z(\mu)$*

Another quantity which is needed in Eqs. (3-28) and (3-29) is the product $\varphi(z, \mu) F_z(\mu)$, $0 \leqslant \mu \leqslant 1$, for $z \in [-1, 0]$ and $z = \nu_j$.

For $z \in [-1, 0]$, the definition (3-27) of F_z involves both a Cauchy principal value integral and the X function. However, Eq. (3-27) may be rewritten as

$$F_z(\mu) = \frac{1}{D(z,\mu)} \left\{ \frac{D(z,\mu) - D(z,z)}{z-\mu} (z-\mu) X(\mu) + D(z,z) X(z) \right.$$
$$+ (z-\mu) D^0(z,\mu) \int_0^1 d\nu \frac{\gamma(\nu)}{\nu-\mu}$$
$$\left. + (z-\mu) \int_0^1 d\nu \frac{\gamma(\nu)[D^0(z,\nu) - D^0(z,\mu)]}{\nu-\mu} \right\}. \tag{4-15}$$

From Eqs. (4-14) and (3-26) we see that the first and third terms in the right side of the above expression cancel. Then, multiplying by $(cz/2)D(z,\mu)/(z-\mu)$ and using Eqs. (3-8) and (3-25) we find for $z \in [-1, 0]$,

$$\varphi(z,\mu) F_z(\mu)$$
$$= \frac{cz}{2} \left\{ \frac{D(z,z)}{z-\mu} X(z) + \int_0^1 d\nu \frac{\gamma(\nu)[D^0(z,\nu) - D^0(z,\mu)]}{\nu-\mu} \right\}, \qquad 0 \leqslant \mu \leqslant 1. \tag{4-16}$$

This form now involves only regular integrals and $X(\mu)$ for $-1 \leqslant \mu \leqslant 0$.

For $z = \nu_j, j = 1, \ldots, M$, the definition (3-27) of F_z is also difficult to evaluate numerically because of the occurrence of $D(\nu_j, \nu_j)$. Fortunately, it is possible to modify Eq. (3-27) so that it contains only the quantity $D(\nu_j, \mu)$, $-1 \leqslant \mu \leqslant 1$, which can be found from the method of Part C of this section. Using the definition (3-26) of the function D^0 and the identity (4-14) one may verify the relation

$$\varphi(z,\mu) F_z(\mu) = \frac{cz}{2} \frac{1}{z-\mu} \int_0^1 d\nu\, \gamma(\nu) \left\{ \frac{D(z,\mu)}{\nu-\mu} - \frac{D(z,\nu)(z-\mu)}{(\nu-\mu)(z-\nu)} \right\} \tag{4-17}$$

or, equivalently,

$$\varphi(z,\mu) F_z(\mu) = \frac{cz}{2} \frac{1}{z-\mu} \left\{ \int_0^1 d\nu \frac{\gamma(\nu) D(z,\nu)}{\nu-z} - \int_0^1 d\nu \frac{\gamma(\nu)[D(z,\mu) - D(z,\nu)]}{\nu-\mu} \right\} \tag{4-18}$$

which holds for $0 \leqslant \mu \leqslant 1$.

F. *Calculation of the Expansion Coefficients*

Before we can solve numerically Eqs. (3-28) and (3-29) for the coefficients $b_{\pm j}$ and $B_{\pm}(\nu)$, $0 \leqslant \nu \leqslant 1$, the incident distribution $\Psi(\mu)$ of Eq. (2-2) must be specified. We have chosen a delta function incident source, i.e., $\Psi(\mu) = \delta(\mu - \mu_0)$, $\mu_0 > 0$. The solution of the albedo problem for any other incident source can readily be

obtained by convoluting the source function, Ψ, with the solution for the delta function source.

With this particular choice of the incident source function Eq. (3-28) may then be written

$$B_{\pm}(\mu) = W(\mu)\Big\{\frac{2\gamma(\mu_0)}{c\mu D(\mu,\mu_0)}\,\varphi(\mu,\mu_0) - \sum_{j=1}^{M} b_{\pm j}[\varphi(\nu_j,\mu)\,F_{\nu_j}(\mu) \pm e^{-d/\nu_j}\varphi(-\nu_j,\mu)\,F_{-\nu_j}(\mu)] \mp \int_0^1 d\nu\, B_{\pm}(\nu)\, e^{-d/\nu}\varphi_{-\nu}(\mu)\,F_{-\nu}(\mu) + \int_0^1 d\nu\, B_{\pm}(\nu)\,\nu\int_0^1 d\xi\,\frac{\gamma(\xi)\,D^0(\nu,\xi)}{\mu D(\mu,\xi)}\,\varphi_{\mu}(\xi)\Big\}, \quad 0 \leqslant \mu \leqslant 1. \tag{4-19}$$

However, this equation and Eq. (3-29) are not very amenable to numerical analysis since the first term on the right hand side of Eq. (4-19) contains the quantity $\varphi(\mu,\mu_0)$ which is highly singular. If instead of using $B_{\pm}$, a new pair of coefficients $\bar{B}_{\pm}$ is introduced such that

$$B_{\pm}(\mu) = W(\mu)\Big[\frac{2\gamma(\mu_0)}{c\mu D(\mu,\mu_0)}\,\varphi(\mu,\mu_0) + \bar{B}_{\pm}(\mu)\Big], \qquad 0 \leqslant \mu \leqslant 1, \tag{4-20}$$

Eq. (4-19) can then be cast into a form which does not contain any singular functions. We introduce the following abbreviations:

$$p_{\pm kj} = \int_0^1 d\mu\,\mu^k\gamma(\mu)\,\varphi(\nu_j,\mu) \pm e^{-d/\nu_j}\int_0^1 d\mu\,\mu^k\gamma(\mu)\,\varphi(-\nu_j,\mu), \tag{4-21}$$

$$P_{\pm j}(\mu) = \varphi(\nu_j,\mu)\,F_{\nu_j}(\mu) \pm e^{-d/\nu_j}\varphi(-\nu_j,\mu)\,F_{-\nu_j}(\mu), \qquad 0 \leqslant \mu \leqslant 1, \tag{4-22}$$

$$H_{\pm k}(\nu) = W(\nu)\Big[e^{-d/\nu}\int_0^1 d\mu\,\mu^k\gamma(\mu)\,\varphi(-\nu,\mu) \mp \frac{c\nu}{2}\int_0^1 d\mu\,\mu^k\gamma(\mu)\,D^0(\nu,\mu)\Big], \quad 0 \leqslant \nu \leqslant 1, \tag{4-23}$$

$$L_{\pm}(\mu,\nu) = W(\nu)\Big[e^{-d/\nu}\varphi(-\nu,\mu)\,F_{-\nu}(\mu) \mp \nu\int_0^1 d\xi\,\frac{\gamma(\xi)\,D^0(\nu,\xi)}{\mu D(\mu,\xi)}\,\varphi(\mu,\xi)\Big], \quad 0 \leqslant \nu \leqslant 1,\ 0 \leqslant \mu \leqslant 1, \tag{4-24}$$

$$J_{\pm k} = \oint_0^1 d\nu\,\frac{H_{\pm k}(\nu)}{\nu-\mu_0} + \frac{2H_{\pm k}(\mu_0)\,\lambda(\mu_0)}{c\mu_0 D(\mu_0,\mu_0)} = \int_0^1 d\nu\,\frac{H_{\pm k}(\nu) - H_{\pm k}(\mu_0)}{\nu-\mu_0} + H_{\pm k}(\mu_0)\Big\{\frac{2\lambda(\mu_0)}{c\mu_0 D(\mu_0,\mu_0)} + \ln\frac{1-\mu_0}{\mu_0}\Big\}, \tag{4-25}$$

and

$$J_{\pm}(\mu) = \int_0^1 d\nu \, \frac{L_{\pm}(\mu, \nu)}{\nu - \mu_0} + \frac{2L_{\pm}(\mu, \mu_0)\,\lambda(\mu_0)}{c\mu_0 D(\mu_0, \mu_0)},$$

$$= \int_0^1 d\nu \, \frac{L_{\pm}(\mu, \nu) - L_{\pm}(\mu, \mu_0)}{\nu - \mu_0} + L_{\pm}(\mu, \mu_0)\left\{\frac{2\lambda(\mu_0)}{c\mu_0 D(\mu_0, \mu_0)} + \ln\frac{1 - \mu_0}{\mu_0}\right\}$$

$$0 \leqslant \mu \leqslant 1. \quad (4\text{-}26)$$

With these definitions Eqs. (3-29) and (4-19) may be written in terms of $\bar{B}_{\pm}$ as

$$\sum_{j=1}^{M} b_{\pm j} p_{\pm kj} \pm \int_0^1 d\nu \, \bar{B}_{\pm}(\nu)\, H_{\pm k}(\nu) = \gamma(\mu_0)[{\mu_0}^k - J_{\pm k}], \qquad k = 0, 1, \ldots, (M-1) \quad (4\text{-}27)$$

and

$$\bar{B}_{\pm}(\mu) + \sum_{j=1}^{M} b_{\pm j} P_{\pm j} \pm \int_0^1 d\nu \, \bar{B}_{\pm}(\nu)\, L_{\pm}(\mu, \nu) = \mp\gamma(\mu_0)\, J_{\pm}(\mu), \quad 0 \leqslant \mu \leqslant 1, \quad (4\text{-}28)$$

respectively. All of the quantities defined in Eqs. (4-21) to (4-26) are readily evaluated, except perhaps $L_{\pm}(\mu, \nu)$ which requires the evaluation of an integral of a singular function (i.e., $\varphi(\mu, \xi)$). However, use of Eqs. (3-8), (4-14) and (3-24) gives

$$L_{\pm}(\mu, \nu) = W(\nu)\left\{e^{-d/\nu}\varphi(-\nu, \mu)\, F_{-\nu}(\mu) \pm \frac{c\nu}{2}\int_0^1 d\xi \, \frac{\gamma(\xi)[D^0(\nu, \xi) - D^0(\nu, \mu)]}{\xi - \mu}\right\}. \quad (4\text{-}29)$$

Finally, to solve Eqs. (4-27) and (4-28) for $b_{\pm j}$ and $\bar{B}_{\pm}$, once the quantities $p_{\pm kj}$, $P_{\pm j}$, $H_{\pm k}$, $L_{\pm}$, $J_{\pm k}$, and $J_{\pm}$ have been found, we approximate the integrals in these equations by quadrature. If $\{\mu_i\}$, $i = 1, \ldots, S$ represents the set of quadrature coordinates for the interval [0, 1], and w_i is the weight function for the i-th coordinate, then the integral equations (4-27) and (4-28) can be approximated by the following set of $2(M + S)$ linear algebraic equations:

$$\sum_{j=1}^{M} b_{\pm j} p_{\pm kj} \pm \sum_{i=1}^{S} w(\nu_i)\, H_{\pm}(\nu_i)\, \bar{B}_{\pm}(\nu_i) = \gamma(\mu_0)[{\mu_0}^k - J_{\pm k}], \qquad k = 0, 1, \ldots, (M-1) \quad (4\text{-}30)$$

and

$$\bar{B}_{\pm}(\mu_i) + \sum_{j=1}^{M} b_{\pm j} P_{\pm j} \pm \sum_{l=1}^{S} w(\nu_l)\, L_{\pm}(\mu_i, \nu_l) = \mp\gamma(\mu_0)\, J_{\pm}(\mu_0), \qquad i = 1, \ldots, S, \quad (4\text{-}31)$$

which may be solved for the $2(M + S)$ unknowns $b_{\pm j}$, $j = 1, \ldots, M$ and $\bar{B}_{\pm}(\mu_i)$, $i = 1, \ldots, S$, e.g., using the method of Crout [17].

Once the quantities $b_{\pm j}$ and $\bar{B}$ have been calculated, the expansion coefficients, $a_{\pm j}$ and A, are readily obtained from them. From Eqs. (3-18), (3-19), and (4-20) we have

$$a_{+j} = \tfrac{1}{2}(b_{+j} + b_{-j}), \tag{4-32}$$

$$a_{-j} = \tfrac{1}{2}(b_{+j} - b_{-j})\, e^{-d/\nu_j}, \tag{4-33}$$

$$A(\mu) = W(\mu)\Big[\frac{2\gamma(\mu_0)\,\varphi(\mu, \mu_0)}{c\mu D(\mu, \mu_0)} + O_1(\mu)\Big], \qquad 0 \leqslant \mu \leqslant 1 \tag{4-34}$$

and

$$A(-\mu) = W(\mu)\, O_2(\mu)\, e^{-d/\mu}, \qquad 0 \leqslant \mu \leqslant 1, \tag{4-35}$$

where we have defined

$$O_1(\mu) = \tfrac{1}{2}\{\bar{B}_+(\mu) + \bar{B}_-(\mu)\} \tag{4-36}$$

and

$$O_2(\mu) = \tfrac{1}{2}\{\bar{B}_+(\mu) - \bar{B}_-(\mu)\}\, e^{-d/\mu}. \tag{4-37}$$

G. *Calculation of the Angular and Scalar Densities and Net Current*

The angular distribution for the slab albedo problem in terms of the coefficients $a_{\pm j}$ and A is given by Eq. (3-17). For computational purposes it is convenient to separate the flux into the "continuous" and "discrete" components, i.e.,

$$\psi(x, \mu) = \psi_d(x, \mu) + \psi_c(x, \mu), \tag{4-38}$$

where

$$\psi_d(x, \mu) = \sum_{j=1}^{M} a_{+j}\varphi(\nu_j, \mu)\, e^{-x/\nu_j} + \sum_{j=1}^{M} a_{-j}\varphi(-\nu_j, \mu)\, e^{x/\nu_j} \tag{4-39}$$

and

$$\psi_c(x, \mu) = \psi_{c1}(x, \mu) + \psi_{c2}(x, \mu) + \psi_{c3}(x, \mu), \tag{4-40}$$

where

$$\psi_{c1}(x, \mu) = \int_0^1 d\nu\; W(\nu)\, O_1(\nu)\, \varphi(\nu, \mu)\, e^{-x/\nu}, \tag{4-41}$$

$$\psi_{c2}(x, \mu) = \int_0^1 d\nu\; W(\nu)\, O_2(\nu)\, \varphi(-\nu, \mu)\, e^{-(d-x)/\nu}, \tag{4-42}$$

and

$$\psi_{c3}(x, \mu) = \int_0^1 d\nu\; \frac{W(\nu)\,\gamma(\mu_0)\,\varphi(\nu, \mu_0)}{\tfrac{1}{2}c\nu D(\nu, \mu_0)}\, \varphi(\nu, \mu)\, e^{-x/\nu}. \tag{4-43}$$

The discrete term ψ_d presents no computational difficulties, and the terms ψ_{c1} and ψ_{c2} likewise are easily evaluated. The third continuum term, ψ_{c3}, while quite straightforward for $\mu < 0$, cannot be evaluated numerically for $\mu > 0$ since the integrand in Eq. (4-43) contains a product of two singular functions, viz., $\varphi(\nu, \mu_0)$ $\varphi(\nu, \mu)$. However, it can be shown [12] that ψ_{c3} may be simplified to

$$\psi_{c3}(x, \mu) = \gamma(\mu_0) \frac{G(x, \mu, \mu) - G(x, \mu, \mu_0)}{\mu - \mu_0} + e^{-x/\mu}\delta(\mu - \mu_0), \qquad \mu > 0, \tag{4-44}$$

where we have defined

$$G(x, \mu, \mu_0) = \frac{c}{2} \oint_0^1 d\nu\, W(\nu)\, e^{-x/\nu} \frac{\nu D(\nu, \mu)}{\nu - \mu_0} + \lambda(\mu_0)\, W(\mu_0)\, \frac{D(\mu_0, \mu)}{D(\mu_0, \mu_0)}\, e^{-x/\mu_0}. \tag{4-45}$$

The last term in the expression (4-44) represents the uncollided flux – that is, the source particles which have penetrated a distance x into the slab without interacting with the medium. For the purposes of computation we can ignore this term since we are really interested only in the angular density established in the slab by the particles which have undergone collisions. Nevertheless, we should keep in mind that the complete solution to the slab albedo problem contains this attenuated delta function.

Finally, the scalar density and net current are determined from the zeroth and first angular moments, respectively, of Eq. (4-38). From Eq. (3-5) and Eqs. (4-38) to (4-43), one finds that the scalar density, ρ, is given by

$$\begin{aligned}\rho(x) = &\sum_{j=1}^{M} [a_{+j}e^{-x/\nu_j} + a_{-j}e^{x/\nu_j}] \\ &+ \gamma(\mu_0) \left\{ \int_0^1 d\nu\, \frac{W(\nu)\, e^{-x/\nu}}{\nu - \mu_0} + \frac{2\gamma(\mu_0)\, W(\mu_0)\, e^{-x/\mu_0}}{c\mu_0 D(\mu_0, \mu_0)} \right\} \\ &+ \int_0^1 d\nu\, W(\nu)[0_1(\nu)\, e^{-x/\nu} - 0_2(\nu)\, e^{-(d-x)/\nu}].\end{aligned} \tag{4-46}$$

The first angular moment of the eigenfunction $\varphi(\nu, \mu)$ is found from Eq. (3-2) and the orthogonality properties of the Legendre polynomials. Combining the result with Eqs. (4-38) to (4-43) one finds that the net current, j, is given by

$$\begin{aligned}j(x) = (1 - c) &\left\{ \sum_{j=1}^{M} \nu_j [a_{+j}e^{-x/\nu_j} - a_{-j}e^{x/\nu_j}] \right. \\ &+ \gamma(\mu_0) \left[\int_0^1 d\nu\, \frac{\nu W(\nu)\, e^{-x/\nu}}{\nu - \mu_0} + \frac{2\gamma(\mu_0)\, W(\mu_0)\, e^{-x/\mu_0}}{cD(\mu_0, \mu_0)} \right] \\ &\left. + \int_0^1 d\nu\, \nu W(\nu)[0_1(\nu)\, e^{-x/\nu} - 0_2(\nu)\, e^{-(d-x)/\nu}] \right\}.\end{aligned} \tag{4-47}$$

V. Numerical Examples

On the basis of the analysis of the preceding section computer programs have been developed to calculate the angular density, scalar density and net current of particles everywhere inside a slab of finite thickness. In this section we present several numerical examples. Specifically, we show how the reflected and transmitted fluxes (i.e., the angular densities at the free surfaces $x = 0$ and $x = d$, respectively) vary with the problem parameters, viz., the degree of anisotropy, N, of the scattering function, the angle of incidence, $\theta_0 = \cos^{-1}\mu_0$, of the source beam, the slab thickness, d, and the multiplication factor, c.

To study the effect of anisotropic scattering it is necessary to specify a particular phase function for single scattering, $f(\Omega' \cdot \Omega)$, cf. Eq. (2-6). For our studies we have used the fictitious function

$$f^{N+}(\Omega' \cdot \Omega) = \frac{N+1}{2^N}(1 + \Omega' \cdot \Omega)^N, \qquad N = 0, 1, 2,.... \tag{5-1}$$

As N increases, f^{N+} becomes concentrated nearer to $\Omega' \cdot \Omega = 1$, corresponding to predominantly forward scattering. While this scattering function is strictly a mathematical invention, f^{N+} is not at all unlike scattering functions encountered in physical situations. For example, in radiative transfer the scattering functions are usually monotonic increasing functions of $\Omega' \cdot \Omega$ (neglecting small backscatter effects) which are highly peaked in the forward direction. In many cases, the function f^{N+} can be used as a good approximation. Mathematically, the function f^{N+} has the advantage that it can be expanded exactly in terms of the first $N + 1$ Legendre polynomials,

$$f^{N+}(\Omega' \cdot \Omega) = \sum_{n=0}^{N} b_n{}^N P_n(\Omega' \cdot \Omega), \tag{5-2}$$

where the coefficients, $b_n{}^N$, can be calculated from the recurrence relation

$$b_n{}^N = \frac{N+1}{2N}\left[\frac{n}{2n-1} b_{n-1}^{N-1} + b_n^{N-1} + \frac{n+1}{2n+3} b_{n+1}^{N-1}\right] \tag{5-3}$$

with $b_0{}^N = 1$ $(N = 0, 1, 2,...)$ and $b_n{}^N = 0$ if $n > N$. In Fig. 1 the scattering function f^{N+} is shown for various degrees of anisotropy.

Finally, we must mention that in all the following examples the incident distribution Ψ of Eq. (2-2) is not simply $\delta(\mu - \mu_0)$ which was used in the analysis of the previous section; rather, we have used

$$\Psi(\mu) = (2\pi\mu_0)^{-1}\,\delta(\mu - \mu_0). \tag{5-4}$$

This particular normalization represents a source beam of constant unit strength

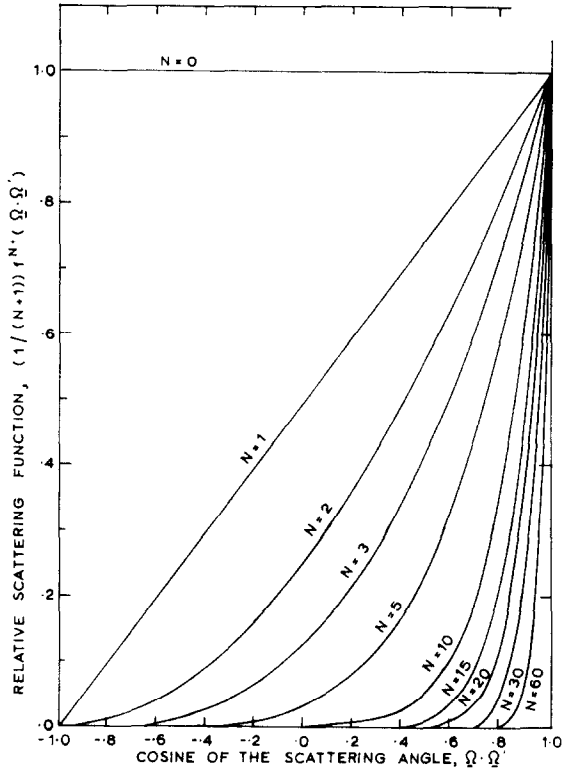

FIG. 1. The scattering function f^{N+} for various degrees of anisotropy.

incident on the slab surface, i.e., a unit incident current. In most experimental situations the source beam strength is indeed kept constant regardless of the angle of incidence, μ_0.

A. *Variation with Degree of Anisotropy*

In Figs. 2 and 3 we show for two different source angles, $\theta_0 = \cos^{-1}\mu_0$, the reflected and transmitted fluxes of a slab of one mean free path thickness and a multiplication factor $c = .95$ for various degrees of anisotropy of the scattering function f^{N+}.

We immediately see that the reflected flux rapidly decreases at all values of $-\mu$ as the degree of forward scattering increases, and more so as the source angle, θ_0, grows smaller. This behaviour is expected since for the particles to be reflected they must change from their initial direction by at least an amount $\mu_0 = \cos\theta_0$ and

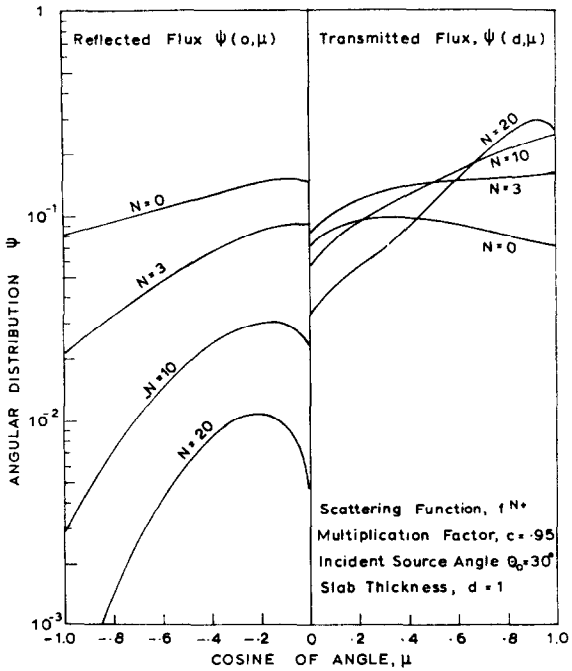

FIG. 2. Reflected and transmitted angular distributions of the slab albedo problem for various degrees of anisotropy.

becomes more forward and as μ_0 increases. Further, the reflected fluxes generally decrease as the emergent angle approaches the perpendicular direction. The principal reason for this is that there is a greater probability for a small change in direction due to collisions than for a large change from the incident direction, particularly as the probability of forward scattering increases. Hence there should be more particles escaping in directions which require only a relatively small change in direction, namely in the direction $\mu \lesssim 0$. Also we will shortly see that the presence of the free surface at $x = d$ contributes to this effect. Finally we notice this increase of the reflected flux as μ increases usually levels off and often decreases slightly as $\mu \to 0$. To understand this effect, which in radiative transfer is known as "limb darkening," consider a particle at some distance x in the slab moving in a negative direction μ_1 towards the surface $x = 0$. The probability that it will reach the surface without suffering another scattering collision or being absorbed is $\exp(-x/\mu_1)$–recall that in the one-speed model, all distances are measured in units of mean free path. Thus, as μ_1 becomes smaller, there is less chance that the particle will emerge without another change in direction, and for small μ_1, this effect is very important. Moreover it is seen that this mechanism becomes even more

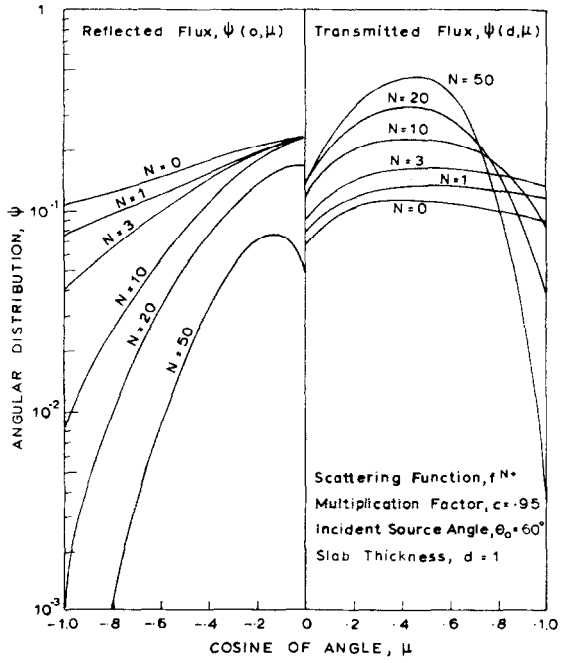

FIG. 3. Reflected and transmitted angular distributions of the slab albedo problem for various degrees of anisotropy.

important as the scattering becomes more and more predominant in the forward direction.

For the transmitted flux, the general trends becomes much more complex and difficult to explain qualitatively. From Figs. 2 and 3 we see the transmitted fluxes generally increase as the forward scattering function f^{N+} becomes more anisotropic. This arises simply because for thin slabs the particles escape after only a few collisions. Indeed, as N increases we see the transmitted flux is peaked nearer to the incident angle, since the particles do not deviate as much from the source direction in only the few collisions they suffer before escaping. The transmitted distribution also become more anisotropic as N increases. Further, these distributions generally display a decrease near $\mu = 0$ (parallel to the surface) probably for the same reasons the reflected flux did near $\mu = 0$.

Finally, we mention the fact that Figs. 2 and 3 provide a means of checking the numerical results since both the reflected and transmitted flux are unaltered when the directions of incidence and emergence are interchanged, as required by Helmholtz's principle of reciprocity [18].

B. *Variation with Slab Thickness*

In Fig. 4 we have plotted the reflected and transmitted fluxes for several slabs of different thicknesses, all with the properties, f^{N+}, $N = 10$, $c = 0.95$, $\theta_0 = 60^0$. The reflected flux, as would be expected, increases as d increases since with larger d there is a smaller probability that the particles will leak through the slab. Also, as d increases the reflected flux falls off less sharply towards the perpendicular direction. This phenomenon is readily understood from the following argument. As d increases, the average number of collisions before a particle escapes increases; hence, the particles can deviate more from their initial direction and may emerge at the surface $x = 0$ with a larger negative angle.

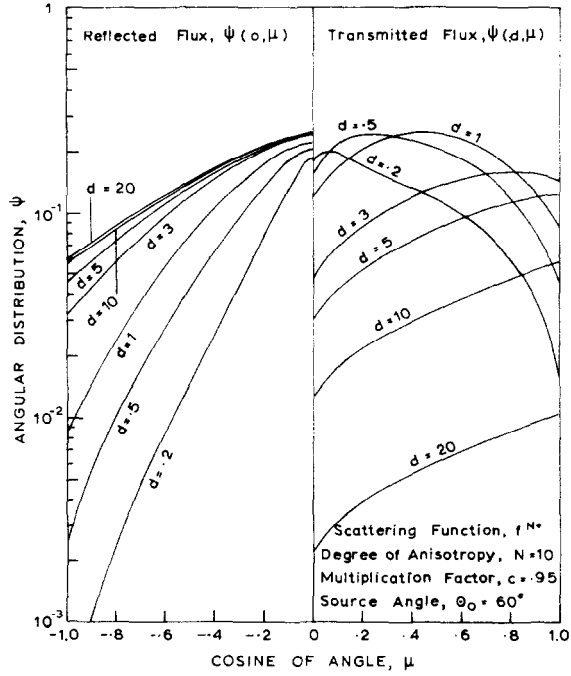

FIG. 4. Reflected and transmitted angular distributions of the slab albedo problem for various slab thicknesses, d.

The transmitted flux initially increases as d increases but then quickly begins to decrease as d becomes still larger. For very small d, very few particles are removed from the source beam and most of the particles are transmitted unaltered (the transmitted delta source is not shown in any of these figures; only the collided flux is displayed). As d increases, more particles are removed from the beam and the transmitted flux increases. However, as d increases further another mechanism

becomes important. At any point in the slab, a particle always has the greatest probability of escaping without suffering another collision when it is moving in a direction perpendicular to either of the free surfaces (i.e., $\mu = +1$ or $\mu = -1$). Eventually, as multiple collisions become more likely as d increases, more particles will be absorbed or scattered into a direction of negative μ (hence the general decrease of the transmitted flux); and the particles traveling in the direction $\mu = 1$ have the greatest chance of reaching the free surface at $x = d$ without being back-scattered or absorbed (hence the transmitted flux attains it largest value at $\mu = 1$).

C. *Variation with Source Angle*

In Figs. 5 and 6 we show how the reflected and transmitted fluxes vary with the source angle, θ_0, for two different cases ($c = 0.95$ and 0.6, respectively) with the same scattering function and slab thickness. We see that the reflected flux rapidly increases for all μ as θ_0 increases. This increase is due to two effects. First, for large θ_0 the source delta function must traverse a distance significantly greater than the slab thickness, d, namely $d/\cos\theta_0$, and hence far more particles will be removed from the source beam than for small θ_0. Secondly, fewer scattering collisions are required to turn the particle into a negative μ direction as θ_0

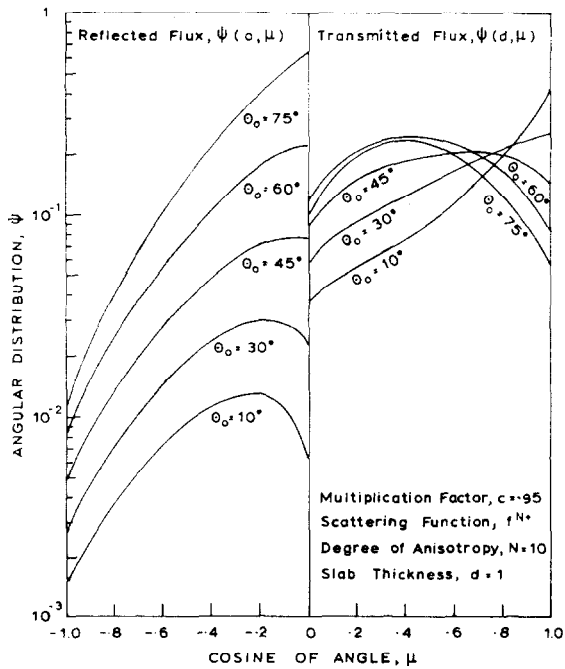

FIG. 5. Variation of the reflected and transmitted angular fluxes with the incident source angle, θ_0, for the slab albedo problem.

is increased and hence more particles will be reflected. The shape of reflected flux distributions, ($\psi(0, \mu)$ increases as μ increases form -1, and then levels off near $\mu = 0$) has been discussed in part A.

The transmitted flux distributions are seen to become more displaced in the perpendicular direction as θ_0 decreases. This simply reflects the fact that the transmission probability is greatest in the direction $\mu = 1$, and as θ_0 decreases fewer collisions are needed to attain this direction. Because in these examples the slabs are so thin that generally very few collisions have occurred in the slab before a particle escapes the transmitted distributions have their maxima between μ_0 and 1. For thicker slabs, more collisions occur and the position of the maxium will shift more from the angle of incidence towards the perpendicular direction.

As with Figs. 2 and 3, the principle of reciprocity may again be invoked to check the numerical results for the reflected and transmitted fluxes represented in Fig. 5 and Fig. 6.

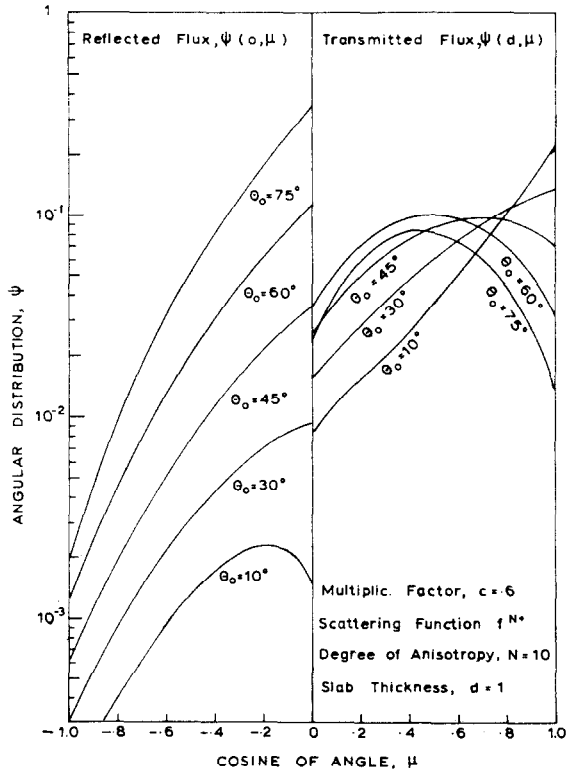

FIG. 6. Variation of the reflected and transmitted angular fluxes with the incident source angle, θ_0, for the slab albedo problem.

D. *Variation with the Multiplication Factor*

Again reference is made to Figs. 5 and 6. The most obvious effect produced by decreasing c is to decrease the transmitted and reflected distributions. This decrease reflects the fact that we have increased the probability of absorption each time the particle has a collision. Hence fewer particles survive removal from the source beam and the subsequent collisions. Further, we notice that the reflected flux decreases more rapidly for decreasing μ when c is decreased — a result of the increased absorption since fewer particles can survive the collisions required to turn them in the $\mu = -1$ direction.

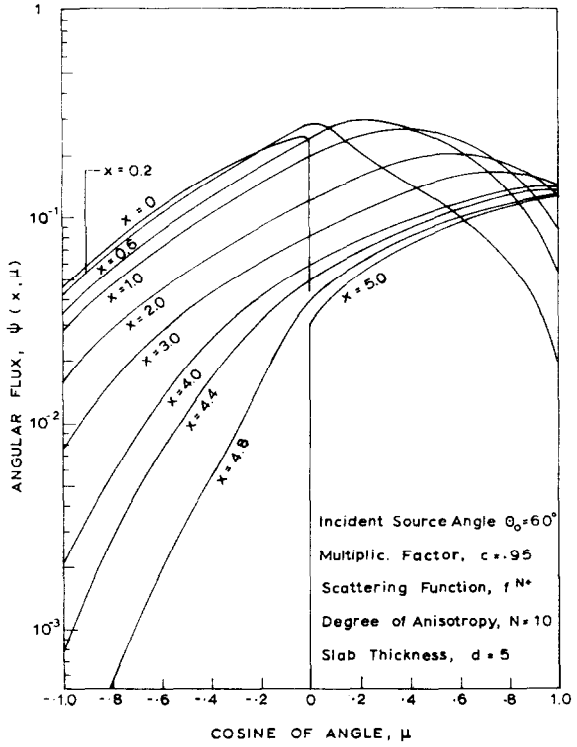

FIG. 7. The angular density for the slab albedo problem at various positions in the slab.

As a final example we show, in Fig. 7, the angular density of particles at several positions inside a slab of 5 mean free paths thickness, with the properties f^{N+}, $N = 10$, $c = 0.95$, $\theta_0 = 60^0$. The value of μ at which the angular density attains its maximum increases as x increases; after a few mean free paths in the slab ($x > 3$) the angular flux becomes a monotonic increasing function of μ. This shift

of the maximum towards the $\mu = 1$ direction for increasing distance in the slab simply reflects the fact that the "real path" distance the particle has traveled to get to a particular point in the slab, is least for the forward direction and, hence, the probability of absorption while traveling to that point is least. Notice also how quickly the angular flux for $\mu > 0$ in the forward direction is established near the source surface, $x = 0$.

Further numerical examples and more details of the computational techniques employed in this research including listings of the computer programs can be found in a recent report [12].

ACKNOWLEDGMENTS

We thank the Computing Center of the University of Groningen for the generous use of its computing facilities during the course of this research.

REFERENCES

1. P. LAFORE AND J. P. MILLOT, Report CEA-1072 (1958).
2. K. M. CASE, *Ann. Phys. New York* **9** (1960), 1.
3. K. M. CASE AND P. F. ZWEIFEL, "Linear Transport Theory," Addison-Wesley, Reading, Mass., 1967.
4. N. J. MCCORMICK AND M. R. MENDELSON, *Nucl. Sci. Eng.* **20** (1964), 462.
5. R. ŽELAŽNY AND A. KUSZELL, *Physica* **27** (1961), 797.
6. I. KUŠČER, N. J. MCCORMICK, AND G. C. SUMMERFIELD, *Ann. Phys. New York* **30** (1964), 411.
7. M. R. MENDELSON, *J. Math. Phys.* **7** (1966), 345.
8. H. G. KAPER, Report TW-37, Mathematisch Instituut, University of Groningen, the Netherlands, 1966.
9. J. K. SHULTIS AND H. G. KAPER, *Astron. Astrophys.* **3** (1969), 110.
10. I. M. GELFAND AND G. E. SCHILOW, "Generalized Functions," Vol. I, Academic Press, Inc., New York, 1964.
11. I. KUŠČER AND I. VIDAV, *J. Math. Anal. Appl.* **25** (1969), 80.
12. H. G. KAPER, J. K. SHULTIS, AND J. G. VENINGA, Report TW-65, Mathematisch Instituut, University of Groningen, the Netherlands, 1969.
13. N. I. MUSKHELISHVILI, "Singular Integral Equations," Noordhoff, Groningen, the Netherlands, 1953.
14. K. M. CASE AND P. F. ZWEIFEL, *J. Math. Phys.* **4** (1963), 1376.
15. A. RALSTON, "A First Course in Numerical Analysis," McGraw-Hill Book Co., New York, 1965.
16. J. K. WILKINSON, *Comput. J.* **3** (1960), 23.
17. L. FOX, *Appl. Math. Ser. U. S. Bur. Stand.* **39** (1954), 1.
18. S. CHANDRASEKHAR, "Radiative Transfer," Dover, New York, 1960.